Quantitative analysis of APP axonal transport in neurons: role of JIP1 in enhanced APP anterograde transport

Kyoko Chiba[a,*], Masahiko Araseki[a,*], Keisuke Nozawa[a,*], Keiko Furukori[a,b], Yoichi Araki[a], Takahide Matsushima[a], Tadashi Nakaya[a], Saori Hata[a], Yuhki Saito[a], Seiichi Uchida[c], Yasushi Okada[d], Angus C. Nairn[b], Roger J. Davis[e], Tohru Yamamoto[f], Masataka Kinjo[g], Hidenori Taru[a], and Toshiharu Suzuki[a]

[a]Laboratory of Neuroscience, Graduate School of Pharmaceutical Sciences, Hokkaido University, Sapporo 060-0812, Japan; [b]Department of Psychiatry, Yale University School of Medicine, New Haven, CT 06508; [c]Human Interface Laboratory, Department of Advanced Information Technology, Faculty of Information Sciences and Electrical Engineering, Kyushu University, Fukuoka 819-0395, Japan; [d]Laboratory for Cell Polarity Regulation, RIKEN Quantitative Biology Center, Suita 565-0874, Japan; [e]Howard Hughes Medical Institute and Program in Molecular Medicine, University of Massachusetts Medical School, Worcester, MA 01605; [f]Department of Molecular Neurobiology, Faculty of Medicine, Kagawa University, Miki-cho 761-0793, Japan; [g]Laboratory of Molecular Cell Dynamics, Faculty of Advanced Life Science, Hokkaido University, Sapporo 001-0021, Japan

ABSTRACT **Alzheimer's β-amyloid precursor protein (APP) associates with kinesin-1 via JNK-interacting protein 1 (JIP1); however, the role of JIP1 in APP transport by kinesin-1 in neurons remains unclear. We performed a quantitative analysis to understand the role of JIP1 in APP axonal transport. In JIP1-deficient neurons, we find that both the fast velocity (~2.7 μm/s) and high frequency (66%) of anterograde transport of APP cargo are impaired to a reduced velocity (~1.83 μm/s) and a lower frequency (45%). We identified two novel elements linked to JIP1 function, located in the central region of JIP1b, that interact with the coiled-coil domain of kinesin light chain 1 (KLC1), in addition to the conventional interaction of the JIP1b 11–amino acid C-terminal (C11) region with the tetratricopeptide repeat of KLC1. High frequency of APP anterograde transport is dependent on one of the novel elements in JIP1b. Fast velocity of APP cargo transport requires the C11 domain, which is regulated by the second novel region of JIP1b. Furthermore, efficient APP axonal transport is not influenced by phosphorylation of APP at Thr-668, a site known to be phosphorylated by JNK. Our quantitative analysis indicates that enhanced fast-velocity and efficient high-frequency APP anterograde transport observed in neurons are mediated by novel roles of JIP1b.**

Monitoring Editor
David G. Drubin
University of California, Berkeley

Received: Jun 17, 2014
Revised: Aug 11, 2014
Accepted: Aug 19, 2014

This article was published online ahead of print in MBoC in Press (http://www.molbiolcell.org/cgi/doi/10.1091/mbc.E14-06-1111) on August 27, 2014.

*These authors contributed equally to this work.

Address correspondence to: Toshiharu Suzuki (tsuzuki@pharm.hokudai.ac.jp).

Abbreviations used: AD, Alzheimer's disease; APP, Alzheimer's β-amyloid precursor protein; GFP, green fluorescent protein; JIP, JNK-interacting protein; JNK, c-Jun NH_2-terminal kinase; KHC, kinesin heavy chain; KLC, kinesin light chain; TPR, tetratricopeptide repeat.

INTRODUCTION

The β-amyloid precursor protein (APP) was identified as the precursor of the amyloid β protein (Aβ), a major component of senile plaques detected in the brains of Alzheimer's disease (AD) patients (Gandy, 2005; Huang and Mucke, 2012). APP is a type I membrane protein, and its C-terminal region can associate with various types of cytoplasmic proteins, including FE65, X11/X11-like proteins, and c-Jun NH_2-terminal kinase (JNK)-interacting proteins (JIPs). These APP-binding partners play an important role in the regulation of APP metabolism and intracellular trafficking (Suzuki and Nakaya, 2008; Thinakaran and Koo, 2008).

JIP1 is an APP-binding partner, and among its isoforms, JIP1b shows the strongest binding affinity for APP (Scheinfeld *et al.*, 2002; Taru *et al.*, 2002). Although JIPs function as scaffold proteins for the JNK signaling cascade (Weston and Davis, 2007), JIP1 has been independently identified as a kinesin light chain (KLC)–binding protein (Verhey *et al.*, 2001; Inomata *et al.*, 2003; Matsuda *et al.*, 2003). Recently JIP1 was found to also associate with kinesin heavy chain (KHC; Fu and Holzbaur, 2013). APP is transported anterogradely by the conventional kinesin-1 motor (Kamal *et al.*, 2000; Araki *et al.*, 2007), which is composed of two KLC and two KHC molecules (Hirokawa *et al.*, 2009; Verhey and Hammond, 2009). With respect to APP cargo transport by kinesin-1, JIP1 plays an important role in kinesin-1 activation (Blasius *et al.*, 2007; Dietrich *et al.*, 2008; Verhey *et al.*, 1998, 2001), although the role of JIP1 in APP anterograde transport is controversial in terms of whether JIP1 regulates APP axonal transport (Fu and Holzbaur, 2013; Vagnoni *et al.*, 2013). Of importance, APP cargo is subject to enhanced axonal transport by kinesin-1 compared with alcadein/calsyntenin cargo, which directly associates with KLC and is transported by kinesin-1 (Konecna *et al.*, 2006; Araki *et al.*, 2007; Kawano *et al.*, 2012). Indeed, the anterograde transport velocity of APP cargo is almost 1.5- to 2-fold greater than that of other kinesin-1 cargoes. The mechanism underlying how APP cargo is transported by kinesin-1 faster than other kinesin-1 cargoes is unclear (Araki *et al.*, 2007), although the possibility that JIP1 activates KHC motility by its direct binding was recently proposed (Fu and Holzbaur, 2013). To understand the precise role of JIP1 in high-speed anterograde transport of APP cargo, more extensive quantitative analysis in living neurons is required.

APP interacts with the phosphotyrosine interaction/phosphotyrosine binding (PI/PTB) domain of JIP through the cytoplasmic NPTY motif in a Tyr phosphorylation–independent manner (Scheinfeld *et al.*, 2002; Taru *et al.*, 2002; Inomata *et al.*, 2003; Suzuki and Nakaya, 2008). The interaction between APP and JIP is considered essential for connection to kinesin-1 (Inomata *et al.*, 2003; Araki *et al.*, 2007), although the direct association of APP with kinesin-1 has been reported (Kamal *et al.*, 2000). In this cargo–motor association, little is known concerning the mechanism of interaction between JIP and KLC. An important study suggested that the 11 C-terminal amino acids (C11) of JIP1 interact with the tetratricopeptide repeat (TPR) motifs within the C-terminal half of KLC1 (Horiuchi *et al.*, 2005), which is the major KLC isoform predominantly expressed in neurons (Niclas *et al.*, 1994).

Understanding how the same motor protein can demonstrate different velocities in response to distinct cargo proteins, such as APP and alcadein, and how cargo proteins regulate motor protein function is of great interest to the field of protein transport and membrane vesicle trafficking. Furthermore, because the regulated intracellular transport of APP cargo is important for the suppression of amyloidogenic APP processing and malfunction of the APP cargo transport system is believed to facilitate the generation of neurotoxic Aβ peptide and/or axonopathy (Stokin *et al.*, 2005; Araki *et al.*, 2007; Morel *et al.*, 2012; Steuble *et al.*, 2012; Vagnoni *et al.*, 2012), understanding the mechanism of anterograde transport of APP cargo by kinesin-1 with quantitative analyses is of particular value. To investigate the properties of anterograde transport of APP cargo by kinesin-1, we dissected the mechanism of interaction between JIP1b and KLC and showed that a series of specific interactions within the APP/JIP1b/kinesin-1 complex is required for highly efficient anterograde transport of APP, which is enhanced by JIP1, in neurons.

RESULTS

JIP1 is essential for the enhanced fast-velocity and efficient high-frequency anterograde transport of APP cargo by kinesin-1

To reveal the role of JIP1 in the enhanced and efficient fast anterograde transport of APP cargo, we analyzed quantitatively the axonal transport of APP cargo in primary cultured mixed cortical/hippocampal neurons from JIP1-KO mice (Whitmarsh *et al.*, 2001). Wild-type ($JIP1^{+/+}$) and JIP1-deficient ($JIP1^{-/-}$) neurons expressing APP-enhanced green fluorescent protein (EGFP) were assayed for APP cargo transport using a total internal reflectance fluorescence (TIRF) microscopy system (Araki *et al.*, 2007). APP cargo was subject to fast anterograde transport (2.73 ± 0.69 μm/s, $n = 533$) in wild-type neurons (Figure 1A and Supplemental Movie S1A) but was transported anterogradely with a reduced average velocity of 1.83 ± 0.49 μm/s ($n = 538$) in neurons lacking JIP1 (Figure 1B and Supplemental Movie S1B; compare B with A; $p < 0.001$). Of note, this reduced rate is almost identical to the speed of alcadein cargoes transported by kinesin-1 (Araki *et al.*, 2007), indicating that JIP1 enhances fast anterograde transport. We excluded stationary vesicles moving at <0.4 μm/s because such vesicles are indistinguishable from those exhibiting Brownian motion. The essential role of JIP1 in the enhanced high-speed velocity of APP cargo was confirmed by expressing FLAG-JIP1b in $JIP1^{-/-}$ neurons, which restored the enhanced fast transport of APP-EGFP (2.68 ± 0.65 μm/s, $n = 96$; Figure 1C and Supplemental Movie S1C; compare C with B; $p < 0.001$).

Of interest, the relative frequency of anterograde transport decreased substantially from 66% in wild-type/$JIP1^{+/+}$ ($n = 121$) to 45% in JIP1-KO/$JIP1^{-/-}$ ($n = 114$) neurons, with the retrograde transport of APP cargo increasing from 10 to 25%. Thus APP cargo is more liable to be transported retrogradely in the absence of JIP1. The level of stationary APP-EGFP vesicles (24% in $JIP1^{+/+}$ neurons) tended to increase slightly in $JIP^{-/-}$ neurons (30%; compare Figure 1, B to A; see insets at right). Exogenous expression of JIP1b in JIP1-deficient neurons restored the ratio of anterograde transport (83%, $n = 64$) above the level observed in wild-type neurons (66%) and decreased the number of stationary vesicles (9%; Figure 1C, right inset). Retrograde transport (8%) of APP-EGFP vesicles was also comparable to the levels observed in wild-type neurons, suggesting an essential role of JIP1 in generating enhanced fast velocity and establishing a higher level of anterograde transport of APP cargo (Table 1), possibly associated with concomitant kinesin-1 activation (Verhey *et al.*, 2001; Blasius *et al.*, 2007).

Slower anterograde transport of APP cargo in JIP1-deficient neurons appears to be due to transport by kinesin-1, because knockdown of KLC-1 expression almost completely abolished anterograde transport of APP cargo (Araki *et al.*, 2007). Although we cannot rule out the possibility that other kinesin superfamily proteins might connect to vesicle cargoes, including APP, it is obvious that nonselective transport of cargo by various motors tends to demonstrate a more diverse distribution in transport velocity, as shown in another quantitative study using artificial transmembrane protein cargoes (Kawano *et al.*, 2012). Therefore it is reasonable to conclude that either the enhanced anterograde transport of APP cargo in the presence of JIP1 or the slower transport in the absence of JIP1 is largely due to kinesin-1.

Role of JNK and APP phosphorylation in enhanced fast-velocity and efficient high-frequency APP anterograde transport

JIP1 is a scaffold protein that associates JNK and its upstream protein kinases in the JNK signaling cascade (Dickens *et al.*, 1997;

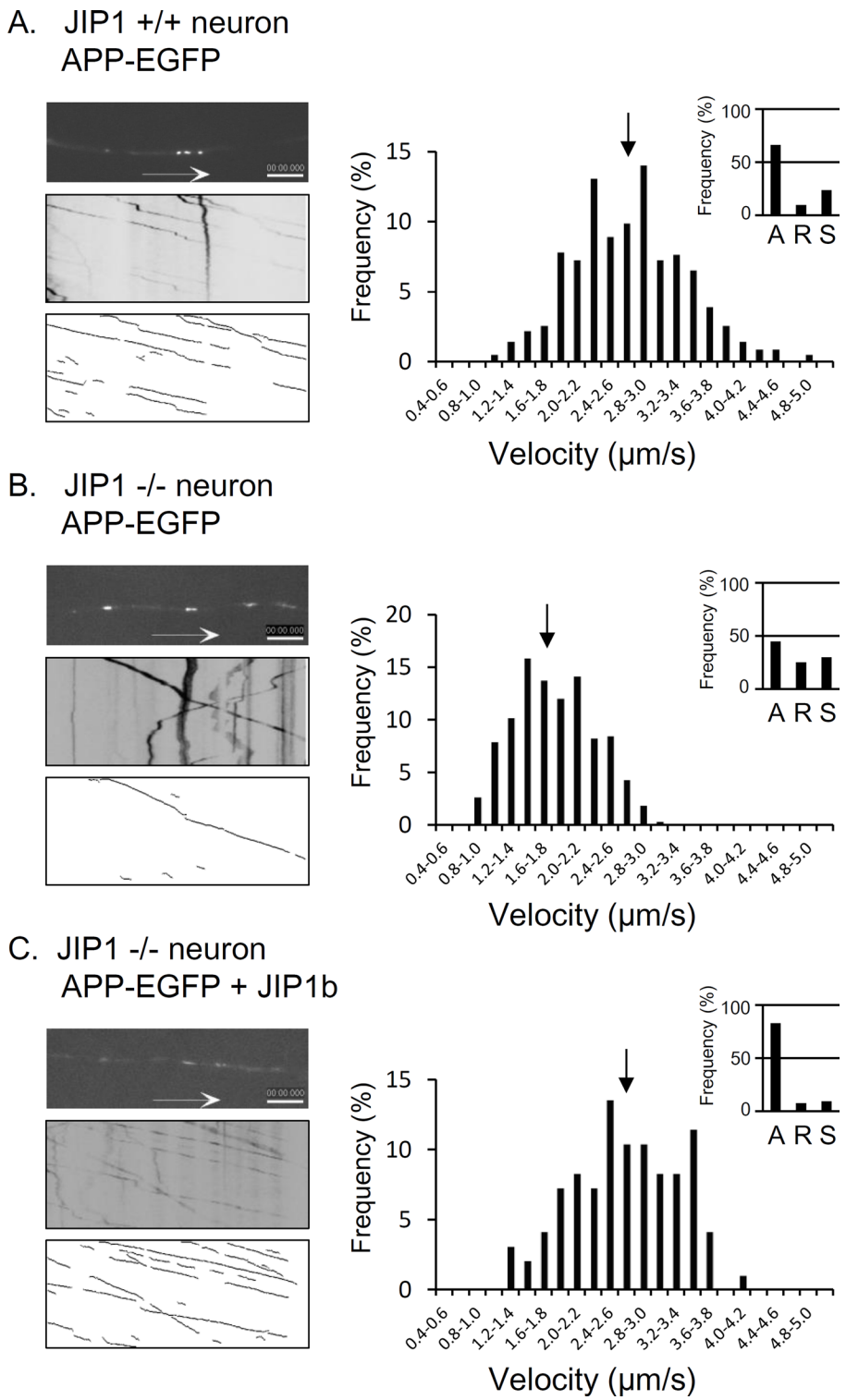

FIGURE 1: JIP1-dependent anterograde transport of APP cargo with enhanced fast velocity and efficient high frequency. APP-EGFP was expressed in primary cultured neurons from wild-type (A) or JIP1-KO (B, C) mice. JIP1b was exogenously expressed in neurons from JIP1-KO mice (C). The transport of APP cargo is shown with movies (left, top; see also supplemental movies), kymographs showing all vesicle movement (left, middle), and the traces of vesicles undergoing only anterograde transport (left, bottom). The cumulative frequencies of velocities (right) of anterograde transport of APP cargo are shown (data are normalized as percentages, and the position of the average velocity is indicated with an arrow). The ratios of anterograde (A), retrograde (R), and stationary (S) vesicles are indicated in the insets at the right. See Supplemental Movie S1A for A, S1B for B, and S1C for C. Scale bar, 5 μm. Statistical analysis for direction of movement vesicles is summarized in Table 1.

Taru *et al.*, 2002). We therefore examined a possible role of JNK and the phosphorylation of APP at Thr-668, which is mediated by protein kinases, including JNK (Taru *et al.*, 2002; Taru and Suzuki, 2004; Inomata *et al.*, 2003; Suzuki and Nakaya, 2008). JIP1-deficient (JIP1$^{-/-}$) neurons expressing APP-EGFP were quantitatively assayed for APP transport after expression of various JIP1b mutants (Figure 2). Expression of JIP1b lacking the PI domain (JIP1bΔPI), which cannot bind to APP (Supplemental Figure S1B), resulted in impaired fast velocity of anterograde transport of APP cargo (average velocity of 1.53 ± 0.18 μm/s, n = 106) compared with that observed in Figure 1C. Anterograde transport frequency was also decreased (53%, n = 36), and retrograde transport was increased to 25%, with the level of stationary cargo remaining unchanged at 22% (Figure 2A and Supplemental Movie S2A). The frequency of anterograde transport was similar to that observed in JIP1$^{-/-}$ neurons (Figure 1B), indicating that the interaction between APP and JIP1 is required for efficient APP anterograde transport.

In contrast, expression of JIP1b carrying amino acid substitutions at Arg-156 and Pro-157 (JIP1b$^{R156G/P157G}$), which cannot bind JNK (Nihalani *et al.*, 2003; Supplemental Figure S1C), restored enhanced fast velocity of anterograde APP transport to a level observed in wild-type JIP1b$^{+/+}$ neurons (average velocity of 2.89 ± 0.56 μm/s, n = 157; Figure 2B and Supplemental Movie S2B). Furthermore, the frequency of anterograde transport was also moderately restored (60%, n = 40). However, JIP1b$^{R156G/P157G}$ expression in JIP1$^{-/-}$ neurons did not decrease the level of stationary APP cargoes (30% of stationary vesicles in Figure 2B; see Table 1). This last observation might suggest some role of JNK in the activation of stationary APP cargo. A possible mechanism by which JIP1 phosphorylation by JNK regulates KHC activation was recently reported (Fu and Holzbaur, 2013).

We also examined the role of APP phosphorylation, using primary cultured neurons derived from the APP^{T668A} mouse, in which Thr-668 of endogenous APP was replaced with Ala-668 to mimic the nonphosphorylated form of APP (Sano *et al.*, 2006; Matsushima *et al.*, 2012). APP^{T668A}-EGFP expressed in neurons from APP^{T668A} knock-in mice was anterogradely transported with enhanced fast velocity (2.82 ± 0.73 μm/s, n = 263) and efficient high frequency (59%, n = 34) comparable to that of APP-EGFP in wild-type neurons (66%; compare Figure 2C with Figure 1A and Supplemental Movie S2C with Supplemental Movie S1A). The ratios

Comparison	A	R	S	Figures
JIP1$^{-/-}$ to JIP1$^{+/+}$	***	***	N.S.	1B to 1A
JIP1$^{-/-}$ to JIP1$^{-/-}$ (JIP1b)	***	**	**	1B to 1C
JIP1$^{-/-}$ to JIP1$^{-/-}$ (JIP1b ΔPI)	N.S.	N.S.	N.S.	1B to 2A
JIP1$^{-/-}$ to JIP1$^{-/-}$ (JIP1b RPG)	N.S.	*	N.S.	1B to 2B
JIP1$^{-/-}$ to JIP1$^{-/-}$ (JIP1b Δ351–514)	N.S.	N.S.	N.S.	1B to 5A
JIP1$^{-/-}$ to JIP1$^{-/-}$ (JIP1b Δ370–402)	N.S.	N.S.	*	1B to 5B
JIP1$^{-/-}$ to JIP1$^{-/-}$ (JIP1b Δ465–483)	N.S.	N.S.	N.S.	1B to 5C
JIP1$^{-/-}$ to JIP1$^{-/-}$ (JIP1b Y705A)	N.S.	*	N.S.	1B to 5D

Results of Figures 1, 2, A and B, and 5 are summarized, with statistical analysis for the ratio of movement directions. APP movement in JIP1$^{-/-}$ neurons is compared with that in JIP1$^{+/+}$ neurons in the first row, and APP movement in JIP1$^{-/-}$ neurons expressing JIP1b proteins is compared with that in JIP1$^{-/-}$ neurons in subsequent rows.
A, anterograde; R, retrograde; S, stationary. *$p < 0.05$; **$p < 0.01$; ***$p < 0.005$. N.S., not significant.

TABLE 1: Summary of statistical analysis for movement direction of APP-GFP vesicles in JIP1$^{-/-}$ neurons.

of retrograde transport (15%) and stationary state (26%) of APP cargoes were also comparable to those of APP transport in wild-type neurons (respectively, 10 and 24%). These results strongly support the conclusion that phosphorylation of APP does not participate in the regulation of enhanced fast-velocity and efficient high-frequency APP anterograde transport in neurons. However, quantitative studies indicate that the interaction of JIP1b with KLC plays a significant role in the regulation of APP anterograde transport efficiency. Therefore we focused our further analysis on the interaction between JIP1b and KLC.

Novel association of the N-terminal half of KLC1 with JIP1b

The role of JIP1b in efficient anterograde transport of APP cargo was examined by detailed analysis of the interaction of JIP1b and KLC1. First, we expressed four region-deleted KLC1 proteins with N-terminal hemagglutinin (HA) or C-terminal EGFP tags in COS7 cells and examined their binding to N-terminal FLAG-JIP1b or FLAG-JIP1bΔC11, the latter lacking the 11 known KLC-binding C-terminal amino acids (schematic protein structures are shown in Figure 3A).

Similar levels of HA-KLC1 (FL), HA-ΔN (lacking 202 N-terminal amino acids), HA-TPR (lacking 200 N-terminal and 48 C-terminal amino acids), and HA-N200 (lacking 342 C-terminal amino acids) were assayed for FLAG-JIP1b binding (Figure 3B). Immunoprecipitates (IPs; lanes 1–8) and cell lysates (lysate; lanes 9–16) were analyzed by immunoblotting with anti-HA and anti-FLAG antibodies. FLAG antibody recovered HA-KLC1 (FL) along with FLAG-JIP1b (lane 1). A comparable amount of HA-TPR and FL was coimmunoprecipitated with FLAG-JIP1b (lane 3). HA-N200, which lacks known JIP1-binding TPR motifs, was moderately coimmunoprecipitated with FLAG-JIP1b (lane 4). Very weak association between ΔN and JIP1b was observed (lane 2).

The interaction between FLAG-JIP1b and KLC1-EGFP (FL) was confirmed by coimmunoprecipitation, but FLAG-JIP1b did not bind C46-EGFP (C-terminal 497–542 region, composed of 46 amino acids) or EGFP alone (Supplemental Figure S1D; see Figure 3A for protein domain structure), supporting the specificity of the interaction between N200 and JIP1b (observed in Figure 3B). However, the 11 C-terminal amino acids of JIP1b (JIP1b C11) are necessary for the interaction with KLC (Verhey *et al.*, 2001). Therefore we examined the association of HA-tagged KLC1, TPR, and N200 to FLAG-tagged JIP1bΔC11 (Figure 3C). Although JIP1bΔC11 failed to bind TPR (lane 5), this deletion mutant bound to N200 (lane 6), as well as to FL KLC1 (lane 4). Intact JIP1b again associated with KLC1 (FL), TPR, and N200 (lanes 1–3), and the immunoprecipitation was specific because no HA-KLC proteins were recovered in the absence of JIP1b expression (lanes 7–9). Taken together, these coimmunoprecipitation assay results indicate that JIP1b interacts with the 200–amino acid N-terminal region of KLC1 without involvement of the 11 C-terminal amino acids.

Detailed analysis of the KLC1-binding site of JIP1b

To identify the novel KLC1-binding region of JIP1b, we performed coimmunoprecipitation of FLAG-tagged JIP1b fragments with HA-tagged KLC1 (FL), TPR, and N200 (Supplemental Figure S2). To stabilize the small JIP1b fragments in cells, some fragments were fused to the C-terminus to EGFP (schematic protein structures are shown in Supplemental Figure S2A). The IPs and lysates were analyzed by immunoblotting with anti-FLAG and anti-HA antibodies (Supplemental Figure S2, B–D), and a summary of the interactions between both proteins is shown (Supplemental Figure S2A, right). KLC1 bound to JIP1b$^{351\text{-}514}$ and JIP1b$^{403\text{-}707}$ to the same extent as intact JIP1b (lanes 1, 3, and 6 in FL, first row of Supplemental Figure S2B, left). TPR bound to JIP1b$^{403\text{-}707}$ (lane 13 in TPR, second row), and N200 bound to JIP1b$^{351\text{-}514}$ and JIP1b$^{403\text{-}707}$ (lanes 17 and 20 in N200, third row) along with intact JIP1b (lane 8 in TPR, second row and lane 15 in N200, third row). As expected, the C-terminal half of JIP1b (JIP1b$^{403\text{-}707}$) associated with TPR (lane 13 of TPR, second row) to the same extent as KLC1 (lane 6 of FL, first row). Of interest, JIP1b$^{351\text{-}514}$ (lane 17) interacted with N200 more strongly than JIP1b including C-terminal 11 amino acids (FL in lane 15 and 403-707 in lane 20). We further examined this influence of the C-terminal region on the interaction between KLC1 N200 and a novel region of JIP1b (Supplemental Figure S3). Interactions of HA-N200 with FLAG-tagged JIP1b$^{351\text{-}696}$ and JIP1b$^{351\text{-}707}$ or with JIP1b$^{403\text{-}696}$ and JIP1b$^{403\text{-}707}$ were examined by coimmunoprecipitation assay. JIP1b$^{351\text{-}696}$ and JIP1b$^{351\text{-}707}$ bound to N200 equally, whereas JIP1b$^{403\text{-}707}$ bound weakly to N200 when compared with JIP1b$^{403\text{-}696}$.

These results indicate that a region of JIP1b$^{351\text{-}514}$ interacts with the N-terminal 200 amino acids of KLC1. We confirmed the binding between JIP1b$^{351\text{-}514}$ and N200 of KLC in vitro in pull-down assays using purified GST-JIP1b fusion and KLC1 proteins (Supplemental Figure S4). GST-JIP1b$^{351\text{-}514}$ bound N200 along with KLC1, whereas GST-JIP1bΔ351–514 failed to bind both N200 and KLC1 proteins. This result confirmed that the region within amino acids 351–514 includes a binding site that interacts with the N-terminal 200 amino acids of KLC1.

To further analyze this interaction, we assayed N-terminal FLAG- and C-terminal EGFP-tagged JIP1b$^{351\text{-}514}$, JIP1b$^{403\text{-}514}$, JIP1b$^{403\text{-}439}$, JIP1b$^{440\text{-}464}$, and JIP1b$^{465\text{-}514}$ fragments for binding to KLC1 (FL), TPR, and N200 (Supplemental Figure S2C). N200 bound to FLAG-JIP1b, JIP1b$^{351\text{-}514}$, JIP1b$^{403\text{-}514}$, and JIP1b$^{465\text{-}514}$ (lanes 17–19 and 22 of N200, third row; note that the band throughout the third row indicates a nonspecific product, and HA-KLC1 N200 detected in lanes 17–19 and 22 moves slightly faster than the nonspecific product; compare this band with that in the third row on the right, lysate), as

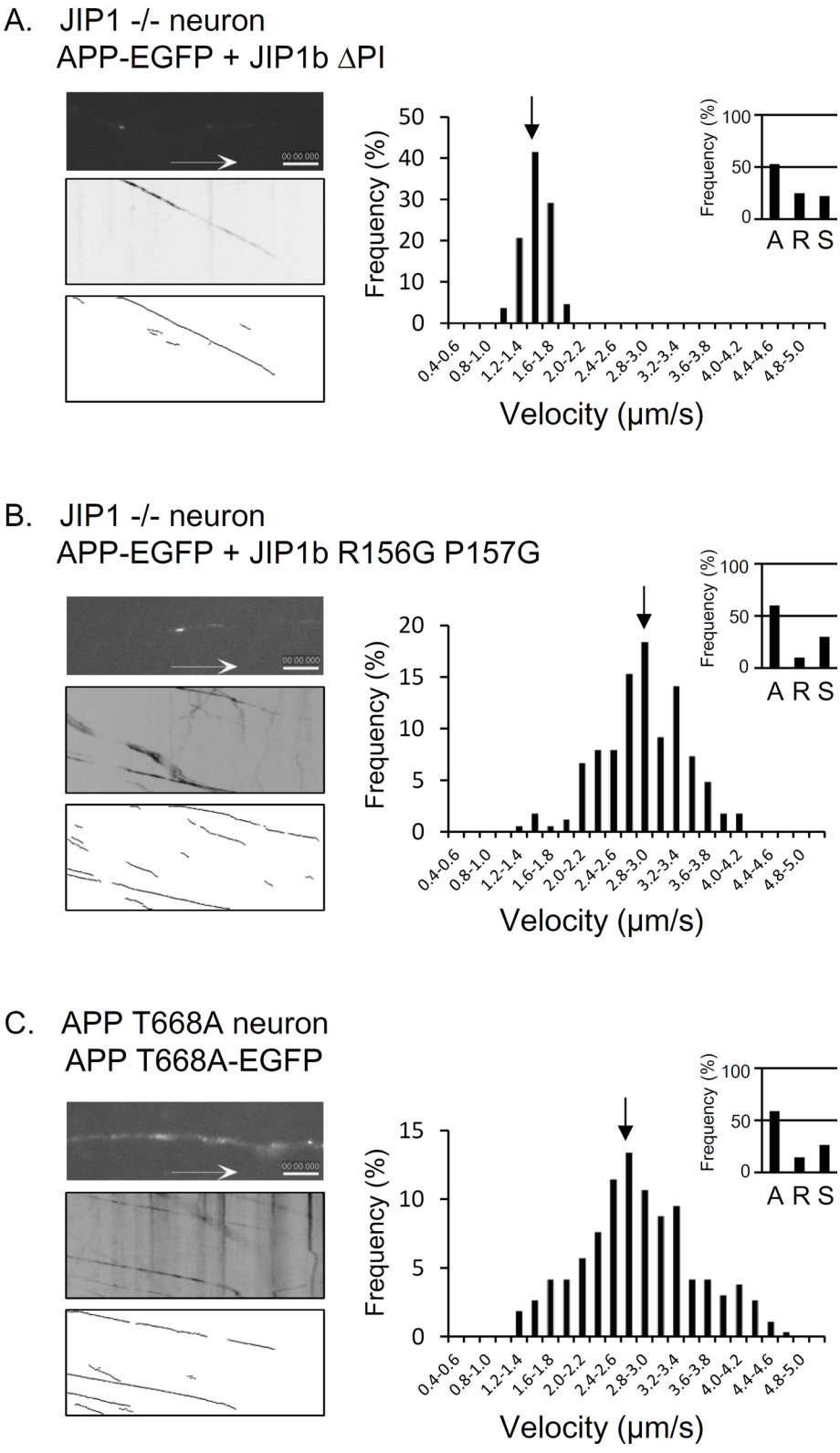

FIGURE 2: JNK binding to JIP1b and APP phosphorylation do not participate in the regulation of efficient anterograde transport of APP cargo. APP-EGFP and the indicated JIP1b mutants were coexpressed in primary cultured neurons from JIP1-KO mice (A, B), and APP T668A-EGFP was expressed in primary cultured neurons from APP T668A-KI mice (C). Data are presented as in Figure 1. The transport of APP cargo is shown. Position of average velocity is indicated with arrows. See Supplemental Movie S2A for A, S2B for B, and S2C for C. Scale bar, 5 μm. The ratios of anterograde (A), retrograde (R), and stationary (S) vesicles are indicated in the insets at the right. Statistical analysis for direction of movement vesicles, except for C, is summarized in Table 1.

well as to intact KLC1 (lanes 1–3 and 6 of FL, first row). The TPR region, as expected, did not bind JIP1b regions within amino acids 351–514 (lanes 10–16 of TPR, second row).

This assay narrowed the KLC1 N200-binding region of JIP1b to amino acids 465–514. We further examined this using N-terminal FLAG- and C-terminal EGFP-tagged JIP1b$^{440-483}$, JIP1b$^{465-483}$, JIP1b$^{484-514}$, and JIP1b$^{465-514}$ fragments. These proteins were assayed for binding to intact KLC1 (FL) and N200 (Supplemental Figure S2D). JIP1b$^{440-483}$ bound to both intact KLC1 and N200 (lane 3 of FL, first row, and lane 10 of N200, second row), as did JIP1b$^{351-514}$ and JIP1b$^{465-514}$ (lanes 1 and 2 of FL, first row, and lanes 8 and 9 of N200, second row). These results indicate that JIP1b$^{440-483}$ includes a region that interacts with the N-terminal half of KLC1.

This novel interaction between JIP1b and KLC was confirmed using region-deleted mutants of JIP1b. Amino acids within or around the 440–483 region of JIP1b were deleted (Supplemental Figure S5A), and the JIP1b deletion mutants were assayed for binding to KLC1, TPR, and N200. N-terminal FLAG-tagged JIP1b, JIP1bΔ440–483, JIP1bΔ465–483, JIP1bΔ351–514, JIP1bΔ440–514, JIP1bΔ403–514, and JIP1bΔ403–483 were expressed in COS7 cells with HA-tagged KLC1 (FL), TPR, and N200, and the cell lysates were subjected to immunoprecipitation with anti-FLAG antibody. The IPs and lysates were analyzed by immunoblotting (Supplemental Figure S5, B and C). As expected, given the presence of the C11 region of JIP1b, intact KLC1 associated with intact JIP1b, JIP1bΔ440–483, and JIP1bΔ465–483 (lanes 1–3 of FL, first row of Supplemental Figure S5B, left). Of interest, TPR did not bind JIP1bΔ440–483 or JIP1bΔ465–483 (lanes 6 and 7 of TPR, second row), regardless of the presence of the C11 region. Moreover, N200 bound JIP1b Δ440–483 and JIP1b Δ465–483 (lanes 10 and 11 of N200, third row), regardless of the absence of the 440–483 region of JIP1b, which is a KLC1 N200-binding site as shown in Supplemental Figure S2.

These observations may be not consistent with our initial conclusion that only JIP1b$^{440-483}$ includes a region that interacts with the N-terminal half of KLC1 (Supplemental Figure S2). Thus, to explain this possible contradiction, we hypothesized that the 440–483 region of JIP1b includes two elements: one is the novel KLC1 N200-binding site, and the other a regulatory element that is required for the interaction between C11 of JIP1b with the TPR motifs of KLC. In addition, JIP1b must possess one more

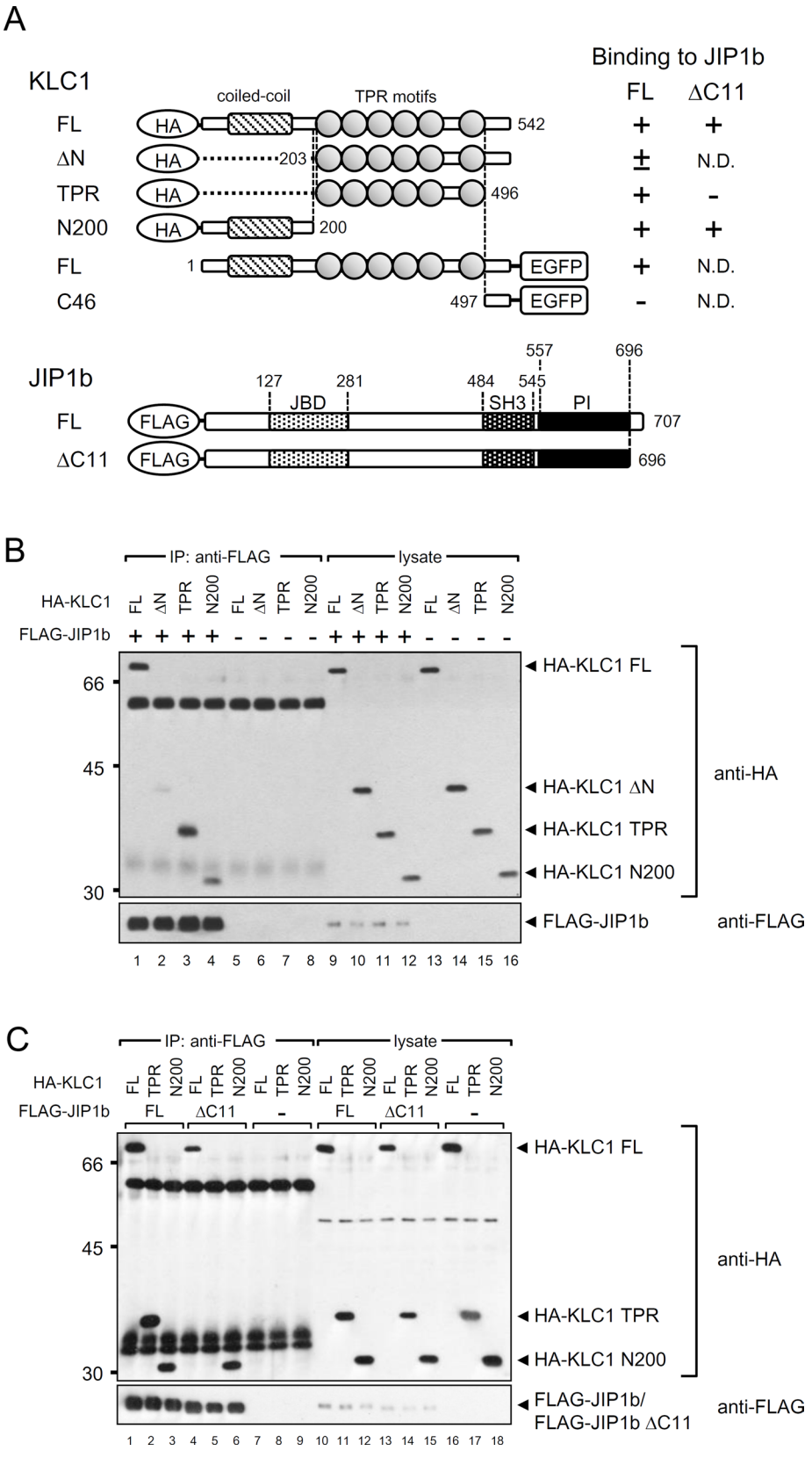

FIGURE 3: Interaction of the N-terminal half of KLC1 with JIP1b. (A) Structure of N-terminal HA- or C-terminal EGFP-tagged mouse KLC1 and N-terminal FLAG-tagged mouse JIP1b proteins. Numbers represent amino acid positions. The shaded box indicates the coiled-coil/heptad repeats region, and ovals indicate TPR motifs in KLC1. JIP1bΔC11 is the truncated protein lacking 11 C-terminal amino acids (^{697}YTCPTEDIYLE^{707}). JBD, JNK-binding motif; SH3, Src homology domain 3; PI, phosphotyrosine interaction or phosphotyrosine binding (PTB) domain. Summary of KLC1 interactions with JIP1b is shown on the right, classified as binding (+), weak binding (±), and nonbinding (–) in a coimmunoprecipitation assay. N.D., not determined. (B, C) Coimmunoprecipitation of KLC1 and JIP1b. The IPs and lysate samples were analyzed by immunoblotting with anti-HA and anti-FLAG antibodies. Numbers shown at the left indicate molecular weight standards (kilodaltons). Numbers shown below indicate lane numbers. Protein bands at ~60 and 35 kDa in the IP lanes shown in this and later figures are derived from the antibody used.

binding site for N200. In other words, N200 can bind to one region within JIP1b$^{440\text{-}483}$ and another region within JIP1b$^{351\text{-}439}$. Furthermore, the 440–483 region also includes a regulatory element required for the interaction, and lack of this regulatory element may negate the conventional association between the TPR of KLC and the C11 of JIP1b.

To examine this possibility, we further analyzed the interaction of KLC1 and N200 with other JIP1b deletion mutants (Supplemental Figure S5C). KLC1 and N200 bound JIP1bΔ440–514, JIP1bΔ403–514, and JIP1bΔ403–483 but not JIP1bΔ351–514, along with intact JIP1b (lanes 1–5 of FL, first row, and lanes 13–17 of N200, third row, Supplemental Figure S5C). This analysis suggests the existence of another N200 binding region within JIP1b$^{351\text{-}402}$. TPR failed to bind all JIP1b deletion proteins (lanes 8–11 of TPR) and only bound intact JIP1b (lane 7 of TPR, second row). The fact that JIP1bΔ465–483 lost its ability to bind to TPR regardless of the preservation of C11 suggests that the 465–483 region of JIP1b includes an element that regulates the interaction of the C11 of JIP1b with the TPR motifs of KLC1.

The region within and around 351–402 of JIP1b was further examined with a series of truncation fragments (see Supplemental Figure S6A). N-terminal FLAG- and C-terminal EGFP-tagged JIP1b fragments JIP1b$^{351\text{-}514}$, JIP1b$^{351\text{-}483}$, JIP1b$^{351\text{-}402}$, JIP1b$^{351\text{-}369}$, and JIP1b$^{370\text{-}402}$ were expressed with HA-tagged intact KLC1 (FL) or N200, and coimmunoprecipitation assays were performed (Supplemental Figure S6, B and C). N200 bound JIP1b$^{351\text{-}514}$, JIP1b$^{351\text{-}483}$, JIP1b$^{351\text{-}402}$ (lanes 6–8 of N200, second row, Supplemental Figure S6B, left), and JIP1b$^{370\text{-}402}$ but interacted very weakly with JIP1b$^{351\text{-}369}$ (lanes 6–8 of N200, second row, Supplemental Figure S6C, left), as did intact KLC1 (lanes 1–3 of FL, first row, Supplemental Figure S6, B and

C). These results indicate that the 370–402 region of JIP1b includes an amino acid sequence that associates with the N-terminal half of KLC1.

To confirm that the two novel binding sites in JIP1b interact with N200, amino acids 370–402 and 465–483, and an element within amino acids 465–483 regulates binding to TPR motifs, we returned to the analysis of the interaction between JIP1b and N200 of KLC1. Various internal deletion JIP1b mutants (Supplemental Figure S7A) were assayed for their association with HA-KLC1, TPR, and N200 by coimmunoprecipitation (Supplemental Figure S7B). Intact KLC1 did not bind to JIP1bΔ351–514 and JIP1bΔ370–402/Δ465–483 (lanes 3 and 7 of FL, first row, Supplemental Figure S7B), but intact KLC1 bound JIP1bΔ370–402, JIP1bΔ440–514, and JIP1bΔ465–483 (lanes 4–6 of FL, first row). Therefore the 465–483 region of JIP1b includes a regulatory element required for KLC1 binding and particularly for the interaction between the C11 of JIP1b and the TPR motifs of KLC1. N200 also demonstrated the same binding pattern as did intact JIP1b (N200, third row, Supplemental Figure S7B, left), confirming that JIP1b$^{370\text{-}402}$ and JIP1b$^{465\text{-}483}$ include binding sites for the N200 region of KLC1. The results of this investigation with internal deletion JIP1b mutants (Supplemental Figure S7) are consistent with the results of binding region assays (Supplemental Figures S2 and S6). The JIP1b^{Y705A} mutant, JIP1bΔ440–514, and JIP1bΔ465–483 did not bind TPR (lanes 10, 13, and 14 of TPR, second row, Supplemental Figure S7B). The result for the Tyr-705 mutant is consistent with a previous study that found that Tyr-705 located within C11 was an essential amino acid that directly interacts with the TPR of KLC1 (Verhey *et al.*, 2001). We detected a weak interaction between the JIP1b^{Y705A} mutant and KLC1 FL, which resulted from a novel interaction between KLC1 and JIP1b$^{370\text{-}402}$.

The various JIP1b mutants used in this study. and their ability to bind to different regions of KLC1 are summarized in Figure 4A. In addition to the known interaction between JIP1b C11 and TPR motifs of KLC1, two novel interactions were found: binding of the 370–402 and 465–483 regions of JIP1b to the N-terminal region of KLC1, which forms a coiled-coil structure. Furthermore, the 465–483 region of JIP1b plays an important role in regulating the association between JIP1b C11 and TPR motifs of KLC1, or possibly in preserving the physiological conformation of JIP1b, to interact with KLC1. A schematic of the interaction between JIP1b and KLC and its regulation is shown in Figure 4B.

Novel roles of JIP1b elements in enhanced fast-velocity and efficient high-frequency APP anterograde transport

Finally, we explored the roles of the various regions of JIP1b in the regulation of the efficiency of anterograde transport of APP cargo. APP-EGFP was expressed in JIP1$^{-/-}$ neurons in the presence of JIP1bΔ351–514, JIP1bΔ370–402, JIP1bΔ465–483 or JIP1b^{Y705A}, and the anterograde transport of APP cargo was analyzed (Figure 5 and Supplemental Movie S3). Expression of JIP1bΔ351–514 resulted in slow velocity (1.79 ± 0.49 μm/s, n = 239) and reduced frequency (44%, n = 53) of APP anterograde transport, along with increased retrograde transport (24%; Figure 5A and Supplemental Movie S3A), similar to these found in JIP1-deficient neurons (Figure 1B and Supplemental Movie S1B). This mutant cannot bind KLC, because the 351–514 region includes both novel KLC-binding regions, 370–402 and 465–483, and deletion of the 465–483 region suppressed the conventional interaction of KLC TPR with JIP1b C11 (Supplemental Figure S7). Thus it was confirmed that JIP1b mediation of the association between APP and KLC plays an important role in efficient APP anterograde transport by kinesin-1.

Expression of JIP1bΔ370–402 restored the enhanced velocity of APP vesicle transport (3.14 ± 0.54 μm/s, n = 151; Figure 5B and Supplemental Movie S3B), indicating that the association with KLC1 mediated by JIP1b$^{370\text{-}402}$ is not a prerequisite for enhanced fast velocity of APP anterograde transport by kinesin-1. Expression of JIP1bΔ370–402 did not restore the frequency of anterograde transport (56%, n = 40) and did not decrease the frequency of retrograde transport (33%). The slight and nonsignificant increase in anterograde transport of APP was due to the decrease of stationary cargo (11%) (compare Figures 5B and 1B). Thus the interaction with KLC mediated by JIP1b$^{370\text{-}402}$ may contribute to the persistence of anterograde transport (i.e., to protection of anterogradely moving vesicles from a retrograde force) but not activation of stationary vesicles.

In contrast to JIP1bΔ370–402, expression of JIP1bΔ465–483 could not restore the enhanced fast velocity of APP vesicle transport (1.84 ± 0.39 μm/s, n = 158), indicating that association of KLC1 via JIP1b$^{465\text{-}483}$ is necessary for the enhancement of fast velocity of APP vesicle transport (Figure 5C and Supplemental Movie S3C). Expression of JIP1bΔ465–483 failed to activate the anterograde transport of stationary APP cargoes (29%, n = 34), but the ratio of retrograde transport decreased (18%). The slightly, but not significantly, restored anterograde transport ratio (53%) is due to the decrease of the retrograde transport rather than the activated transport of the stationary cargoes (compare Figures 5C and 1B). Thus the interaction with KLC1 mediated by JIP1$^{465\text{-}483}$ may contribute to activation of the stationary state of APP cargoes rather than the persistence of a stable anterograde transport of APP cargoes.

Of interest, expression of the JIP1b^{Y705A} mutant, which inhibits the association with TPR motifs of KLC, as does JIP1bΔC11 (Figure 3C and Supplemental Figure S5; Verhey *et al.*, 2001), but retains the ability to bind KLC1 through the novel KLC-binding regions located in JIP1b$^{351\text{-}514}$, could not restore the enhanced velocity of APP cargo in JIP1$^{-/-}$ neurons (1.62 ± 0.37 μm/s, n = 193). However, the frequency of anterograde transport (51%, n = 59) was similar to that in JIP1$^{-/-}$ neurons (Figure 5D and Supplemental Movie S3D; compare to Figure 1B). Thus the association of KLC1 TPR motifs with JIP1b C11 regulates the enhanced fast-velocity APP anterograde transport. Because a JIP1b$^{465\text{-}483}$ element regulates the interaction between KLC TPR motifs and JIP1b C11, it is reasonable to conclude that JIP1b$^{465\text{-}483}$ is involved in the regulation of enhanced fast velocity of APP transport, which is governed by the association of KLC1 TPR motifs with JIP1b C11. In other words, the novel interaction between JIP1b$^{465\text{-}483}$ and KLC1 N-terminal region is a prerequisite for the conventional association of KLC1 TPR motifs with JIP1b C11. Of interest, the JIP1b^{Y705A} mutant seems to preserve the anterograde transport of APP cargo because of decreased retrograde transport (12%, n = 59) but not to allow the continuous anterograde transport, as shown by the intermittent shorter traces of vesicle movement (see lower kymograph trace in Figure 5D). Furthermore, expression of JIP1b^{Y705A} could not activate the transport of stationary APP cargo (37%; compare Figures 5D and 1, B and C). The effects of JIP1b^{Y705A} expression are similar to those of JIP1bΔ465–483, suggesting that interaction of KLC1 TPR with JIP1b C11, including Tyr-705 is regulated by interaction of the KLC1 N-terminal region with JIP1b$^{465\text{-}483}$, leading to the highly efficient anterograde transport of APP cargo (Table 1).

Finally, we confirmed that the interaction of JIP1bΔC11 or JIP1b^{Y705A} with KLC1 can form a kinesin-1 complex, including KHC (Supplemental Figure S8). FLAG-JIP1bΔC11 coprecipitated KHC in the presence of HA-KLC1, as did FLAG-JIP1b (Supplemental Figure S8A), and KHC-FLAG also coprecipitated HA-JIP1b^{Y705A} in

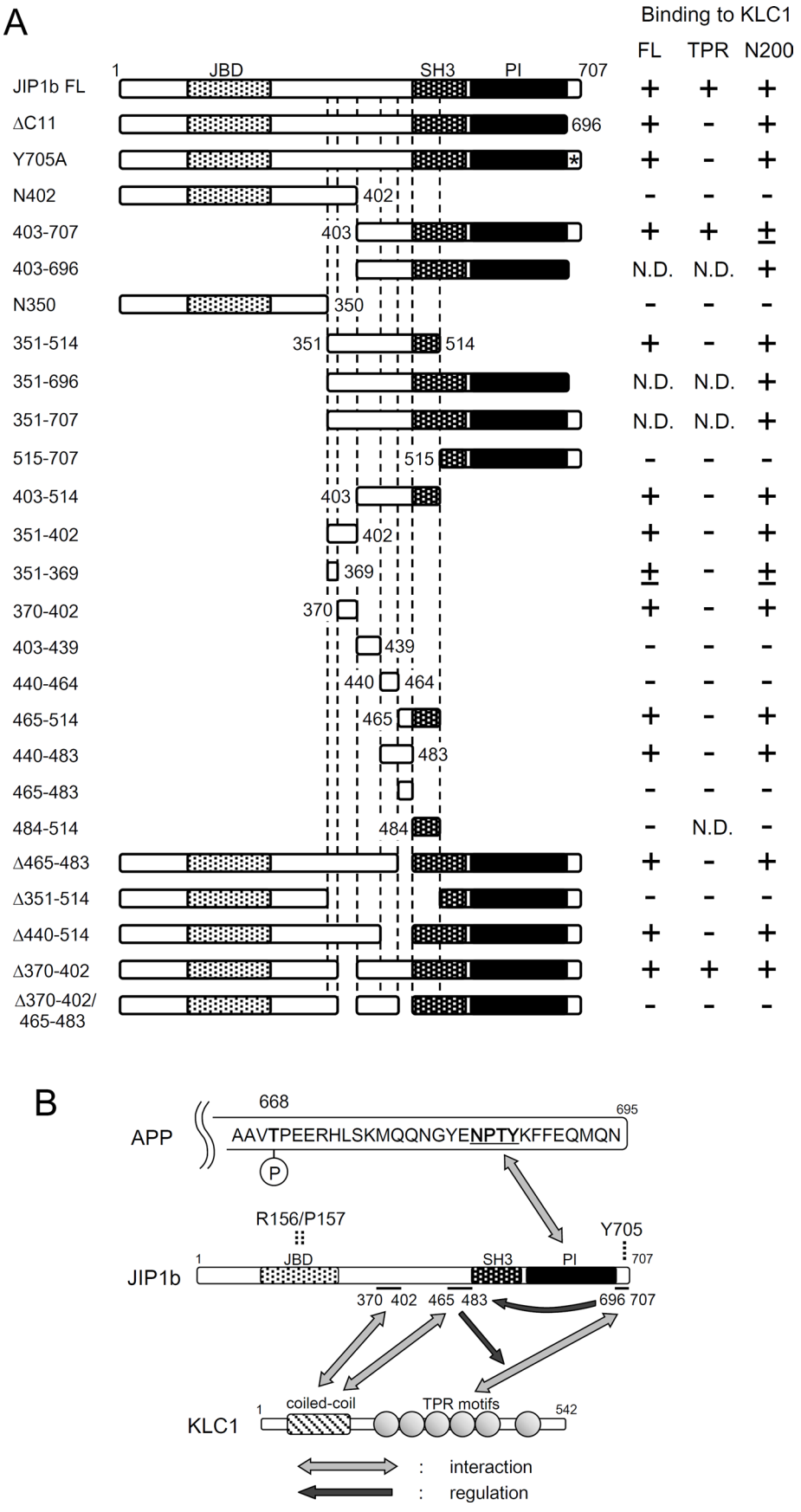

FIGURE 4: Summary of binding between JIP1b and KLC1, and schematic interactions between APP, JIP1b, and KLC. (A) Structures of JIP1b used in this study. Numbers represent amino acid positions. The asterisk indicates the position of alanine substitution for tyrosine (Y705A).

Summary of JIP1b interactions with KLC1 (FL), KLC1 TPR domains (TPR), and the KLC1 N200 region (N200) is shown on the right, classified as binding (+), weak binding (±), and nonbinding (–). N.D., not determined. (B) Schematic interaction between the APP cytoplasmic region, JIP1b, and KLC. The NPTY motif of APP binds to the PI/PTB domain of JIP1b. Thr-668 in APP (numbering for APP695 isoform) is subject to phosphorylation. The 11 C-terminal amino acids of JIP (^{697}YTCPTEDIYLE^{707}), including Tyr-705, interact with the C-terminal half of KLC1, including the TPR motifs. The JIP1b$^{370-402}$ and JIP1b$^{465-483}$ regions were identified as novel binding sites for the N-terminal half of KLC1, including the coiled-coil/heptad repeats. The JIP1b$^{465-483}$ region also showed regulatory activity in the interaction between the 11 C-terminal amino acids of JIP1b and the C-terminal half of KLC1. The C11-terminal region of JIP1b may be involved in the interaction between JIP1b$^{465-483}$ and the N-terminal half of KLC1.

the presence of Myc-KLC1 (Supplemental Figure S8B), indicating that JIP1bΔC11 and JIP1b^{Y705A} can associate with kinesin-1. In other words, JIP1b lacking the ability to bind to the TPR motifs of KLC1 is included in kinesin-1 complex via a novel interaction between KLC1 N200 and JIP1b$^{370-402}$. This supports the conclusion that the interaction between KLC1 N200 and the novel element 370–402 within JIP1b$^{351–514}$ is minimally sufficient for generation of a functional kinesin-1 complex to transport APP cargo anterogradely, although the conventional interaction between the TPR motifs of KLC1 and the C11, including the Tyr-705 residue of JIP1b, is essential for the *enhanced* fast anterograde transport of APP cargo.

DISCUSSION

Here we report a detailed analysis of the role of JIP1 in the efficient anterograde transport of APP cargo by kinesin-1 with enhanced fast velocity and higher frequency. APP is a cargo of kinesin-1, and JIP1 plays an important role in kinesin-1 activation and association of APP with kinesin-1 (Verhey *et al.*, 2001; Taru *et al.*, 2002; Inomata *et al.*, 2003; Matsuda *et al.*, 2003; Horiuchi *et al.*, 2005; Araki *et al.*, 2007; Fu and Holzbaur, 2013). However, detailed analysis of JIP1 function has been limited.

Our observations indicate that 1) the interaction between the TPR motifs of KLC1 and the C11 region, including Tyr-705 of JIP1b, is essential for the enhanced fast anterograde transport of APP cargo; 2) a novel element within amino acids 370–402 of JIP1b is required for preservation and/or

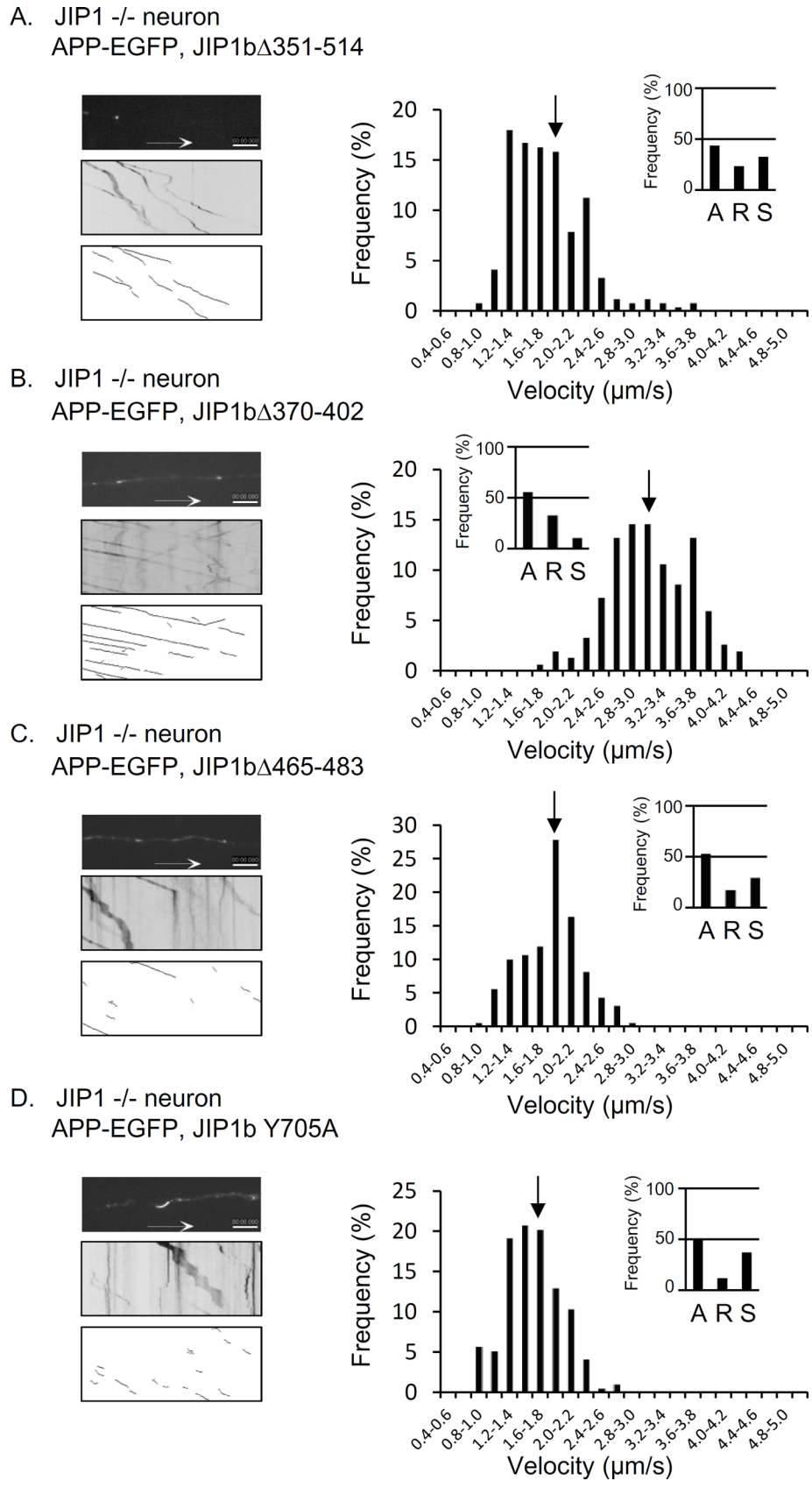

FIGURE 5: Role of novel KLC-binding regions of JIP1b in efficient anterograde transport of APP cargo. APP-EGFP and the indicated JIP1b mutants were expressed in primary cultured neurons from JIP1-KO mice (A–D). Data are presented as in Figure 1. The transport of APP cargo is shown. Position of average velocity is indicated with arrows. See Supplemental Movie S3A for A, S3B for B, S3C for C, and S3D for D. Scale bar, 5 μm. The ratios of anterograde (A), retrograde (R), and stationary (S) vesicles are indicated in the insets at the right. Statistical analysis for direction of movement vesicles is summarized in Table 1.

stabilization of the higher frequency of APP anterograde transport through interaction with the N-terminal region of KLC1; 3) another novel element, amino acids 465–483 of JIP1b, regulates the interaction of the KLC1 TPR domain with the JIP1b C11 domain through an association with the N-terminal region of KLC1; 4) this interaction may also contribute to APP cargo stabilization and/or activation of anterograde transport; and 5) phosphorylation of APP at Thr-668 does not contribute to the increased efficiency of APP cargo transport. The functional interactions among APP, JIP1b, and KLC of kinesin-1 are illustrated in Figure 6.

In the absence of JIP1 or deficiency of JIP1 function, the efficiency of anterograde transport of APP cargo by kinesin-1 is impaired. The lower efficiency of APP cargo transport may in turn impair axonal transport and contribute to neurodegenerative disease. In fact, reduction in kinesin-1 function by KLC1 gene knockout or knockdown impairs axonal transport of APP and induces axonopathy (Stokin *et al.*, 2005; Araki *et al.*, 2007). Kinesin-1 reduction has also been reported in the brains of AD patients (Morel *et al.*, 2012), and a splicing isoform of KLC has been reported as a modifier of Aβ accumulation in brain (Morihara *et al.*, 2013).

A recent report provided evidence for the direct interaction of JIP1 and KHC, which, along with a binding to KLC, activates KHC motility (Fu and Holzbaur, 2013). This aspect of JIP1 function may therefore allow for specific effects of cargoes with KHC. In addition to this hypothesis, our study also proposes another possibility, in which APP cargoes preferentially associate with kinesin-1 through JIP1b when JIP1 is abundant in neurons. However, in the absence of JIP1, APP cargoes presumably bind to kinesin-1 through another unknown mechanism that still allows for fast transport but is less efficient than in the presence of JIP1 (Figure 6). In this respect, we do not rule out the possibility that the APP cargo complex may include other factors, distinct from JIP1, with which APP cargo may be connected to kinesin-1 and transported with reduced velocity.

The JIP1 C11 region has been reported to interact with the TPR motifs of KLC1, and the N-terminal of KLC1 binds to KHC. Amino acid substitution of Ala for Tyr-705 in the C11 region also abolishes the interaction of

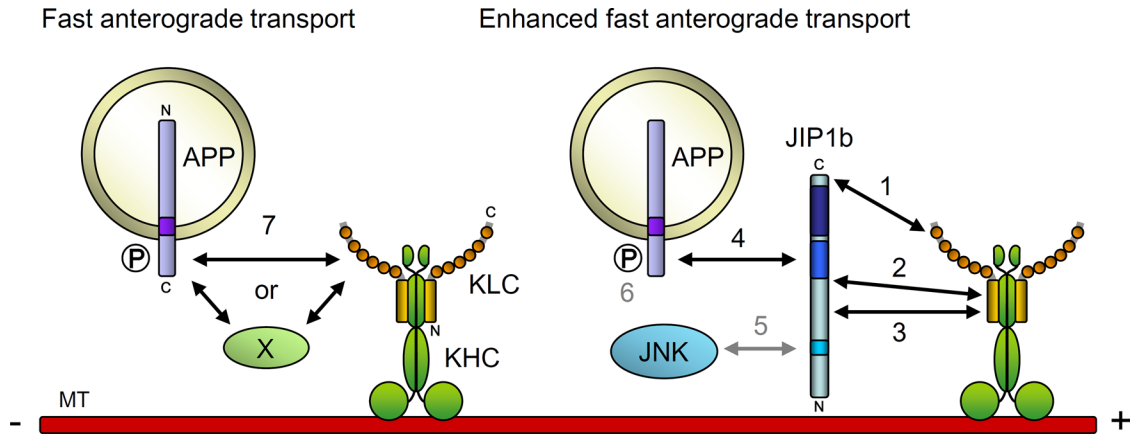

FIGURE 6: Functional interaction between APP, JIP1b, and KLC of kinesin-1. Possible regulation of APP cargo transport by protein interactions is shown schematically. 1) Association of JIP1b C11 to the TPR motif of KLC1 is required for the enhanced fast velocity of anterograde transport of APP cargo. 2) Interaction of JIP1b$^{465\text{-}483}$ with KLC1 N200 regulates the association of JIP1b C11 to the TPR motif of KLC1 and is thus essential for the enhanced fast velocity of anterograde transport of APP cargo. This interaction may also be involved in the decrease of the stationary APP cargo. 3) Interaction of JIP1b$^{370\text{-}402}$ with KLC1 N200 contributes to the stable and higher-frequency anterograde transport of APP cargo. 4) Interaction of the JIP1b PI/PTB domain with the APP cytoplasmic NPTY motif is essential for the enhanced fast velocity and higher frequency of anterograde transport of APP cargo. 5) Interaction of JIP1b JBD with JNK is not involved in the enhanced fast velocity of anterograde transport of APP cargo. 6) Phosphorylation of APP at cytoplasmic Thr^{668} is not involved in the efficient APP anterograde transport by kinesin-1. 7) APP cargoes may interact with kinesin-1 independently of JIP1 to be transported anterogradely with slower velocity. An unknown factor, X, may mediate the interaction of APP with kinesin-1, or APP can directly associate with kinesin-1 in the absence of JIP1.

JIP1 with the TPR motifs of KLC1 (Verhey *et al.*, 2001). The present study revealed that the conventional interaction of the JIP1b C11 region with the TPR motifs of KLC alone is not sufficient to generate efficient axonal anterograde transport of APP cargo with both enhanced fast velocity and higher frequency. Furthermore, the interaction between JIP1b and KLC1 is more complex than previously thought (Figures 4B and 6). In this study we found that the known interaction between JIP1 C11 and TPR motifs of KLC1 is regulated by a novel interaction of JIP1$^{465\text{-}483}$ with N200 of KLC1. Although the conformation of the JIP1-KLC1 complex has not been revealed sufficiently, the interaction of JIP1$^{465\text{-}483}$ with N200 of KLC1 may stabilize structurally the interaction of JIP1 C11 with TPR motifs of KLC1. The existence of JIP1b C11 (695–707 region) affects the interaction between N200 of KLC and JIP1b$^{403\text{-}707}$, including the 465-483 region (Supplemental Figures S2 and S3). Thus two regions, 465–483 and 695–707, of JIP1 may be working together to regulate the interaction with KLC1.

With regard to enhanced fast velocity, there are several possibilities. JIP1 may affect kinesin-1 structure and enhance processive activity as a catalyst in several ways (Toprak *et al.*, 2009) to support faster velocity transport. Alternatively, JIP1 may recruit more kinesin-1 or activate KHC motility (Fu and Holzbaur, 2013). Our study shows that JIP1 enables both enhanced faster movement and preserves anterograde transport of APP cargoes and identifies novel functional regions in JIP1b. In another report (Fu and Holzbaur, 2013), the lack of JIP1 was also found to decrease retrograde transport. In this study, JIP1 also was found to associate in a novel way with the dynein complex. The relationship of any possible interaction of JIP1 and dynein to our results is not clear. In the absence of JIP1, our results showed that there was an increase in retrograde APP transport. However, compared with the major phenotype that the anterograde velocity of APP transport is dramatically reduced in the absence of JIP1, a difference in minor phenotypes related to an increase or a decrease in stationary or retrogradely moving cargoes may depend on the type of neurons and experimental conditions, such as use of neurons derived from CNS or peripheral DRG neurons or neurons derived from the gene knockout mouse or the knockdown study of JIP protein expression by small interfering RNA.

We also show that the JNK-binding region of JIP1b is not involved in the enhanced fast velocity of anterograde transport of APP cargo. Therefore we addressed the role of APP phosphorylation by JNK. APP is subject to phosphorylation at Thr-668 in a neuron-specific manner by several protein kinases, including JNK (Iijima *et al.*, 2000; Taru *et al.*, 2002; Sano *et al.*, 2006; Suzuki and Nakaya, 2008), and this phosphorylation induces conformational and functional changes in the APP cytoplasmic domain (Ando *et al.*, 2001; Ramelot and Nicholson, 2001; Matsushima *et al.*, 2012). However, we clearly demonstrated that the phosphorylation of APP at Thr-668 is not required for enhanced APP anterograde transport by kinesin-1. Instead, we find that novel elements of JIP1b function in the control of efficient anterograde transport of APP cargo by kinesin-1 in neurons. This regulatory role of JIP1b is likely to be critical for efficient anterograde transport of APP, and, further, may be important for preventing neurodegenerative diseases such as Alzheimer's disease.

MATERIALS AND METHODS

Plasmid, cell culture, primary cultured neurons, and coimmunoprecipitation

The original plasmids, including mouse KLC1 and JIP1b cDNA, have been described (Taru *et al.*, 2002; Araki *et al.*, 2007), and mutant plasmids were prepared by PCR technology and subcloned into pcDNA3.1. The KHC plasmid was provided by K. J. Verhey, University of Michigan Medical School, Ann Arbor, MI (Verhey *et al.*, 1998). African green monkey kidney COS7 cells were cultured, and the indicated plasmids were transiently transfected as described (Taru *et al.*, 2002). Preparation of cell lysates has been described (Araki *et al.*, 2007), and the lysates and their immunoprecipitates were subjected to immunoblot analysis with the

indicated antibodies and detected with ECL Plus reagent (GE Healthcare, Wauwatosa, WI).

The primary culture of mixed mouse cortical and hippocampal neurons was performed with a modified version of the method described by Bartlett and Banker (1984). C57BL/6 wild-type and JIP1-KO and APP^{T668A}-KI mice on a C57BL/6 genetic background were used; both lines of mutant mice were previously described (Whitmarsh *et al.*, 2001; Sano *et al.*, 2006). In brief, the cortex and hippocampus of mice at embryonic day 15.5 were dissected, and neurons were spread in a buffer containing papain and cultured at 5 $\times 10^4$ cells/cm^2 in a medium composed of Neurobasal Medium (Life Technologies) containing 30% (vol/vol) Nerve-Cell Culture Medium (DS Pharma Biomedical, Osaka Japan), 2% (vol/vol) B-27 Supplement (Invitrogen, Carlsbad, CA), Glutamax I (4 mM), heat-inactivated horse serum (5% vol/vol), and antibiotics (Invitrogen) on poly-D-lysine–treated glasses. At in vitro day 4, the neurons were transfected with plasmids and cultured for 12 h for analysis with TIRF microscopy. All of the animal studies were conducted in compliance with the guidelines of the Animal Studies Committee of Hokkaido University. All mice were housed in an SPF environment.

Anti-FLAG (M2; Sigma Aldrich, St. Louis, MO), anti-HA (12CA5; Roche, Indianapolis, IN), anti-GFP (MBL, Nagoya, Japan), anti-KLC1 (V-17; Santa Cruz Biotechnology, Santa Cruz, CA), and anti-KHC (H2; Millipore, Temecula, CA) antibodies were obtained commercially as indicated.

TIRF microscopy analysis

Vesicular transport in living neuronal cells was observed using a TIRF microscopy system (C1; Nikon, Tokyo, Japan) with a charge-coupled device camera (Cascade 650; Photometrics, Tucson, AZ). The velocity of anterograde transport was analyzed quantitatively as described in the Supplemental Information of Araki *et al.* (2007). Statistical analysis among cargo velocity distributions was performed with the chi-square test, and the average velocity (indicated with an arrow in the histograms) is shown ±SD. The direction of moving vesicles was further followed by residual analysis. Cargo vesicles presented in the TIRF area, that is, within ~100 nm of the plasma membrane, were counted using the "count objects" function of MetaMorph 6.1. The proportion (percentage) of anterograde and retrograde vesicles relative to the indicated total number of vesicles is shown as "frequency," as described by Araki *et al.* (2007).

Kymographs of moving vesicles in axons (top of kymographs in the figures) and the traces of individual vesicles undergoing anterograde transport (bottom of kymographs) were assembled with the application KymoMaker (Chiba *et al.*, 2014; open access tool at www.pharm.hokudai.ac.jp/shinkei/Kymomaker.html).

In vitro pull-down assay

Glutathione *S*-transferase (GST)-JIP1bΔ351-514, GST alone, GST-KLC1 (FL), and GST-KLC1 N200 (N200) were produced in *Escherichia coli* BL21 (DE3) by expression of pGEX4T1-JIP1b$^{351-514}$, pGEX4T1-JIP1bΔ351-514, pGEX4T1, pGEX4T1-KLC1, and pGEX4T1-KLC1^{N200} vectors. Protein lysates were incubated with glutathione-Sepharose 4B beads and processed as described (Araki *et al.*, 2007). KLC1 and KLC1 N200 were eluted from beads by removing GST after cleavage by thrombin. GST-JIP1b$^{351-514}$, GST-JIP1bΔ351-514, and GST alone were eluted from beads with a buffer including glutathione. The purified GST-fusion proteins were incubated with purified KLC1 proteins, and associated proteins were recovered with glutathione beads. After the beads were washed, proteins were recovered by boiling in SDS-sample buffer and subjected to Western blot analysis with the indicated antibodies.

ACKNOWLEDGMENTS

This work was supported in part by Grants-in-Aid for Scientific Research 22659011, 23390017, and 23113701 to T.S., 23790069 to Y.S., and 24790062 to S.H. from the Ministry of Education, Culture, Sports, Science and Technology (MEXT), Japan, and in part by the Asian Core Program of the Japan Society for the Promotion of Science. A.C.N. was supported by National Institutes of Health Grant AG 09464. S.H. was supported by Bilateral Joint Research Projects of the Japan Society for the Promotion of Science.

REFERENCES

Ando K, Iijima K, Elliott JI, Kirino Y, Suzuki T (2001). Phosphorylation-dependent regulation of the interaction of amyloid precursor protein with Fe65 affects the production of β-amyloid. J Biol Chem 276, 40353–40361.

Araki Y, Kawano T, Taru H, Saito Y, Wada S, Miyamoto K, Kobayashi H, Ishikawa HO, Ohsugi Y, Yamamoto T, *et al.* (2007). The novel cargo Alcadein induces vesicle association of kinesin-1 motor components and activates axonal transport. EMBO J 26, 1475–1486.

Bartlett WP, Banker GA (1984). An electron microscopic study of the development of axons and dendrites by hippocampal neurons in culture. I. Cells which develop without intercellular contacts. J Neurosci 4, 1944–1953.

Blasius TL, Cai D, Jih GT, Toret CP, Verhey KJ (2007). Two binding partners cooperate to activate the molecular motor Kinesin-1. J Cell Biol 176, 11–17.

Chiba K, Shimada Y, Kinjo M, Suzuki T, Uchida S (2014). Simple and direct assembly of kymographs from movies using KYMOMAKER. Traffic 15, 1–11.

Dickens M, Rogers JS, Cavanagh J, Raitano A, Xia Z, Halpern JR, Greenberg ME, Sawyers CL, Davis RJ (1997). A cytoplasmic inhibitor of the JNK signal transduction pathway. Science 277, 693–696.

Dietrich KA, Sindelar CV, Brewer PD, Downing KH, Cremo CR, Rice SE (2008). The kinesin-1 motor protein is regulated by a direct interaction of its head and tail. Proc Natl Acad Sci USA 105, 8938–8943.

Fu MM, Holzbaur EL (2013). JIP1 regulates the directionality of APP axonal transport by coordinating kinesin and dynein motors. J Cell Biol 202, 495–508.

Gandy S (2005). The role of cerebral amyloid beta accumulation in common forms of Alzheimer disease. J Clin Invest 115, 1121–1129.

Hirokawa N, Noda Y, Tanaka Y, Niwa S (2009). Kinesin superfamily motor proteins and intracellular transport. Nat Rev Mol Cell Biol 10, 682–696.

Horiuchi D, Barkus RV, Pilling AD, Gassman A, Saxton WM (2005). APLIP1, a kinesin binding JIP-1/JNK scaffold protein, influences the axonal transport of both vesicles and mitochondria in Drosophila. Curr Biol 15, 2137–2141.

Huang Y, Mucke L (2012). Alzheimer mechanisms and therapeutic strategies. Cell 148, 1204–1222.

Iijima K, Ando K, Takeda S, Satoh Y, Seki T, Itohara S, Greengard P, Kirino Y, Nairn AC, Suzuki T (2000). Neuron-specific phosphorylation of Alzheimer's β-amyloid precursor protein by cyclin-dependent kinase 5. J Neurochem 75, 1085–1091.

Inomata H, Nakamura Y, Hayakawa A, Takata H, Suzuki T, Miyazawa K, Kitamura N (2003). A scaffold protein JIP-1b enhances amyloid precursor protein phosphorylation by JNK and its association with kinesin light chain 1. J Biol Chem 278, 22946–22955.

Kamal A, Stokin GB, Yang Z, Xia CH, Goldstein LS (2000). Axonal transport of amyloid precursor protein is mediated by direct binding to the kinesin light chain subunit of kinesin-I. Neuron 28, 449–459.

Kawano T, Araseki M, Araki Y, Kinjo M, Yamamoto T, Suzuki T (2012). A small peptide sequence is sufficient for initiating kinesin-1 activation through part of TPR region of KLC1. Traffic 13, 834–848.

Konecna A, Frischknecht R, Kinter J, Ludwig A, Steuble M, Meskenaite V, Indermuhle M, Engel M, Cen C, Mateos JM, *et al.* (2006). Calsyntenin-1 docks vesicular cargo to kinesin-1. Mol Biol Cell 17, 3651–3663.

Matsuda S, Matsuda Y, D'Adamio L (2003). Amyloid beta protein precursor (AbetaPP), but not AbetaPP-like protein 2, is bridged to the kinesin light chain by the scaffold protein JNK-interacting protein 1. J Biol Chem 278, 38601–38606.

Matsushima T, Saito Y, Elliott JI, Iijima-Ando K, Nishimura M, Kimura N, Hata S, Yamamoto T, Nakaya T, Suzuki T (2012). Membrane-microdomain localization of amyloid beta-precursor protein (APP) C-terminal

fragments is regulated by phosphorylation of the cytoplasmic Thr668 residue. J Biol Chem 287, 19715–19724.
Morel M, Heraud C, Nicaise C, Suain V, Brion JP (2012). Levels of kinesin light chain and dynein intermediate chain are reduced in the frontal cortex in Alzheimer's disease: implications for axoplasmic transport. Acta Neuropathol 123, 71–84.
Morihara T, Hayashi N, Yokokoji M, Akatsu H, Silverman MA, Kimura N, Sato M, Saito Y, Suzuki T, Yanagida K, *et al*. (2013). Transcriptome analysis of distinct mouse strains reveals kinesin light chain-1 splicing as an amyloid β accumulation modifier. Proc Natl Acad Sci USA 111, 2638–2643.
Niclas J, Navone F, Hom-Booher N, Vale RD (1994). Cloning and localization of a conventional kinesin motor expressed exclusively in neurons. Neuron 12, 1059–1072.
Nihalani D, Wong HN, Holzman LB (2003). Recruitment of JNK to JIP1 and JNK-dependent JIP1 phosphorylation regulates JNK module dynamics and activation. J Biol Chem 278, 28694–28702.
Ramelot TA, Nicholson LK (2001). Phosphorylation-induced structural changes in the amyloid precursor protein cytoplasmic tail detected by NMR. J Mol Biol 307, 871–884.
Sano Y, Nakaya T, Pedrini S, Takeda S, Iijima-Ando K, Iijima K, Mathews PM, Itohara S, Gandy S, Suzuki T (2006). Physiological mouse brain Abeta levels are not related to the phosphorylation state of threonine-668 of Alzheimer's APP. PLoS One 1, e51.
Scheinfeld MH, Roncarati R, Vito P, Lopez PA, Abdallah M, D'Adamio L (2002). Jun NH2-terminal kinase (JNK) interacting protein 1 (JIP1) binds the cytoplasmic domain of the Alzheimer's beta-amyloid precursor protein (APP). J Biol Chem 277, 3767–3775.
Steuble M, Diep TM, Schatzle P, Ludwig A, Tagaya M, Kunz B, Sonderegger P (2012). Calsyntenin-1 shelters APP from proteolytic processing during anterograde axonal transport. Biol Open 1, 761–774.
Stokin GB, Lillo C, Falzone TL, Brusch RG, Rockenstein E, Mount SL, Raman R, Davies P, Masliah E, Williams DS, *et al*. (2005). Axonopathy and transport deficits early in the pathogenesis of Alzheimer's disease. Science 307, 1282–1288.
Suzuki T, Nakaya T (2008). Regulation of amyloid beta-protein precursor by phosphorylation and protein interactions. J Biol Chem 283, 29633–29637.
Taru H, Iijima K, Hase M, Kirino Y, Yagi Y, Suzuki T (2002). Interaction of Alzheimer's beta-amyloid precursor family proteins with scaffold proteins of the JNK signaling cascade. J Biol Chem 277, 20070–20078.
Taru H, Suzuki T (2004). Facilitation of stress-induced phosphorylation of beta-amyloid precursor protein family members by X11-like/Mint2 protein. J Biol Chem 279, 21628–21636.
Thinakaran G, Koo EH (2008). Amyloid precursor protein trafficking, processing, and function. J Biol Chem 283, 29615–29619.
Toprak E, Yildiz A, Hoffman MT, Rosenfeld SS, Selvin PR (2009). Why kinesin is so processive. Proc Natl Acad Sci USA 106, 12717–12722.
Vagnoni A, Glennon EB, Perkinton MS, Gray EH, Noble W, Miller CC (2013). Loss of c-Jun N-terminal kinase-interacting protein-1 does not affect axonal transport of the amyloid precursor protein or Abeta production. Hum Mol Genet 22, 4646–4652.
Vagnoni A, Perkinton MS, Gray EH, Francis PT, Noble W, Miller CC (2012). Calsyntenin-1 mediates axonal transport of the amyloid precursor protein and regulates Abeta production. Hum Mol Genet 21, 2845–2854.
Verhey KJ, Hammond JW (2009). Traffic control: regulation of kinesin motors. Nat Rev Mol Cell Biol 10, 765–777.
Verhey KJ, Lizotte DL, Abramson T, Barenboim L, Schnapp BJ, Rapoport TA (1998). Light chain-dependent regulation of Kinesin's interaction with microtubules. J Cell Biol 143, 1053–1066.
Verhey KJ, Meyer D, Deehan R, Blenis J, Schnapp BJ, Rapoport TA, Margolis B (2001). Cargo of kinesin identified as JIP scaffolding proteins and associated signaling molecules. J Cell Biol 152, 959–970.
Weston CR, Davis RJ (2007). The JNK signal transduction pathway. Curr Opin Cell Biol 19, 142–149.
Whitmarsh AJ, Kuan CY, Kennedy NJ, Kelkar N, Haydar TF, Mordes JP, Appel M, Rossini AA, Jones SN, Flavell RA, *et al*. (2001). Requirement of the JIP1 scaffold protein for stress-induced JNK activation. Genes Dev 15, 2421–2432.